

Supplement S2

SUMMARY

This part of the supplementary material includes a more detailed presentation of the methods used to compare the simulation data with theoretical predictions and a short discussion on the finite size effects in the system.

DATA ANALYSIS

In this section, we present a detailed description of how data were obtained from simulations and compared to the theoretical results obtained in Supplement S1.

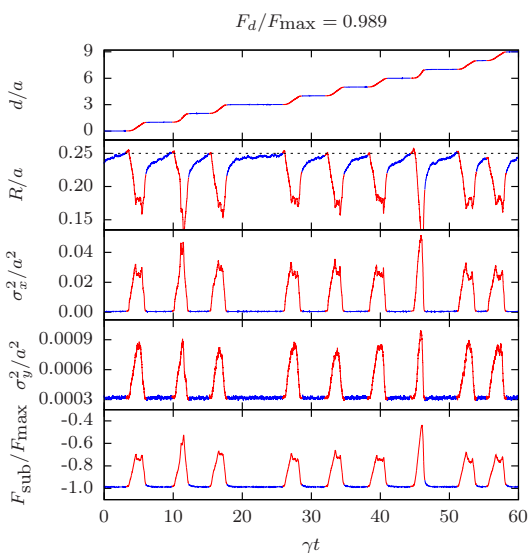


FIG. 1. Total displacement (first panel), periodic center of mass (second panel), variance of the relative displacements of particles, \mathbf{u}_i , in the x and y directions (third and fourth panels), and the net substrate force acting on the monolayer (fifth panel), all plotted as a function of time for part of a trajectory. The inter-particle interaction strength is $\Gamma/k_B T = 1.147$ and the driving force $F_d/F_{\max} = 0.989$. The data points are plotted in blue if the monolayer is undergoing a buildup phase.

As a representative example, we use a part of the trajectory of a monolayer with $\Gamma/k_B T = 1.147$, driven by a force $F_d/F_{\max} = 0.989$. Standard trajectories used for the article were twice as long as the fragment considered here. Similar to the main article, Figure 1 presents the total displacement, the periodic center of mass, the variances of the particle positions, and the net substrate force acting on the monolayer. Data drawn in blue belong to the build up phase, whereas data belonging to configurations in which a hopping wave is traveling through it are colored in red. The periods of rapid motion (hopping waves) are characterized either by the rapid change of

total displacement (top) or spikes in all of the remaining quantities. The buildup phase coincides with plateaus in the total displacement and regions with relatively small changes in other quantities. We used the arbitrarily cut-off, $\sigma_x^2/a^2 < 0.85 \times 10^{-4}$ in order to differentiate between the two phases.

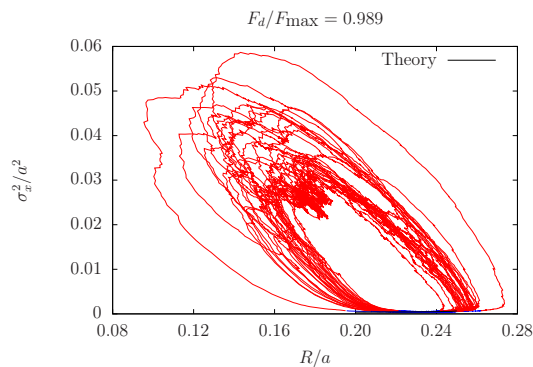


FIG. 2. Variance of the relative displacements of particles, \mathbf{u}_i , in the x direction, σ_x^2 , as a function of the periodic position of the center of mass, R . The inter-particle interaction strength is $\Gamma/k_B T = 1.147$ and the driving force $F_d/F_{\max} = 0.989$.

As can be seen in Figure 2, where σ_x^2 is plotted as a function of the periodic position of the center of mass, values that correspond to the buildup phase are all bundled in a small region of R . In Figure 3, we zoomed in on this region and present σ_x^2 , σ_y^2 and F_{sub} , all as a function of R . The theoretical predictions of the mean value of these quantities has been plotted next to the data. Furthermore, our theory predicts that, in the buildup phase, these distributions are independent of the applied driving force. In Figure 4, we compare the simulation results for a trajectory of a monolayer driven by $F_d/F_{\max} = 0.987, 0.989$, and 1.002 with the theoretical prediction. Evidently, the distributions of the substrate forces of these monolayers overlap strongly.

We have plotted, in Figure 5, a histogram of the net substrate force $F_{\text{sub}}(R)$ acting on the monolayer with the intention not only to show that the theoretical prediction is very close to its expectation value, but that the distribution is also very narrow. As a result, one can, to a good approximation, use $F_{\text{eff}}(R)$ as the effective substrate force acting on the monolayer.

So far, we have only considered driving forces $F_{\max} > F_d > F_{\max}^{\text{eff}}$, where F_{\max}^{eff} is the maximum restoring force of $F_{\text{eff}}(R)$. In this parameter regime, the monolayer is able to drift up to $R = 0.25a$, but also remain in quasi-static equilibrium as it does so. If the driving force is below F_{\max}^{eff} , the monolayer gets pinned by the effective substrate at the position R_0 such that $F_{\text{eff}}(R_0) + F_d = 0$. The monolayer then oscillates about R_0 for a while un-

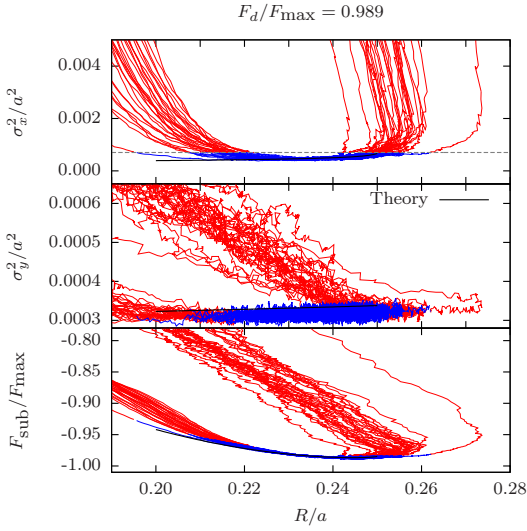


FIG. 3. Variances of the relative displacements of particles, \mathbf{u}_i , in the x and y directions and the net substrate force acting on the monolayer as a function of the periodic position of the center of mass, R , restricted the buildup phase. The inter-particle interaction strength is $\Gamma/k_B T = 1.147$ and the driving force $F_d/F_{\text{max}} = 0.989$. The theoretical predictions are indicated by the solid black lines. The threshold value of σ_x^2 used to differ between the phases is denoted by the dashed gray line which is located at $\sigma_x^2/a^2 = 8.5 \times 10^{-4}$.

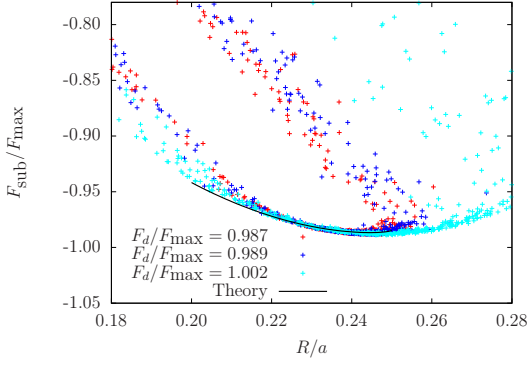


FIG. 4. Net substrate force acting on the monolayer driven by $F_d/F_{\text{max}} = 0.987, 0.989$, and 1.002 as a function of the periodic position of the center of mass, R . The inter-particle interaction strength is $\Gamma/k_B T = 1.147$. The theoretical prediction is indicated by the solid black line.

til a small group of particles spontaneously form a critical “hopping cluster” (red particles in the video) which then initiates a hopping wave. In Figure 6, we have plotted the position of the periodic center of mass for the monolayer with $\Gamma/k_B T = 1.147$, driven at rates below $F_{\text{max}}^{\text{eff}}/F_{\text{max}} = 0.9867$. Using our analytical formula for $F_{\text{eff}}(R)$, we found the corresponding value of R_0 numerically and plotted it as the black dashed line in the graph. Each of the monolayers oscillates for a while about R_0 before creating a hopping wave, as predicted.

For the results presented in the article, we considered

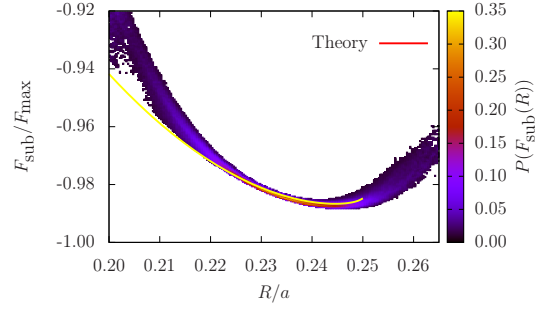


FIG. 5. Distribution of the average substrate forces for multiple buildup phases, gathered from 100 trajectories and several values of the driving forces, as a function of R . The yellow line indicates the theoretical prediction for $F_{\text{eff}}(R)$.

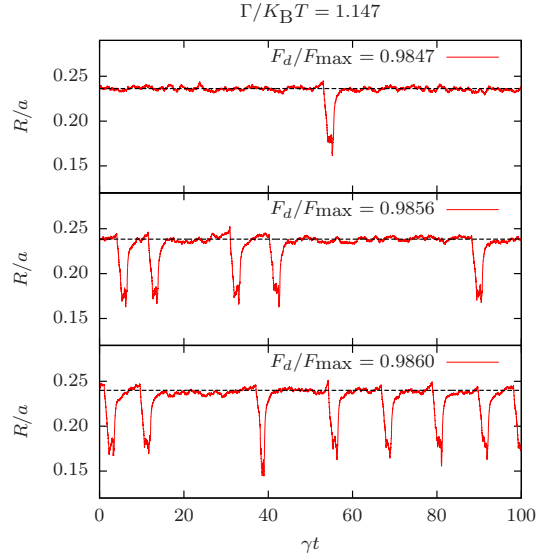


FIG. 6. Periodic center of mass, R , as a function of time for a monolayer driven by $F_d/F_{\text{max}} = 0.9847, 0.9856$, and 0.9860 , all of which are less than $F_{\text{eff}}(\Gamma)$, where $\Gamma/k_B T = 1.147$. Dashed lines indicate theoretical predictions for the position R_0 , at which the monolayers become pinned.

a total of 6 different values of Γ driven with 10 different F_d . For each pair Γ and F_d values, 100 independent trajectories were generated and analyzed.

SYSTEM SIZE DEPENDENCE

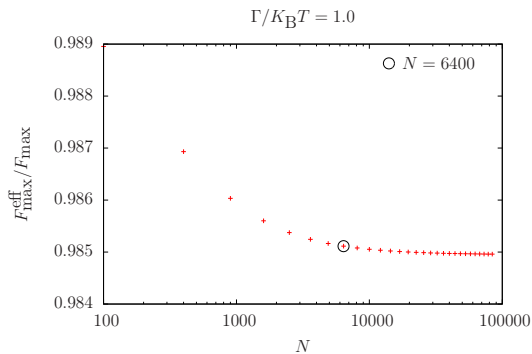


FIG. 7. Theoretical predictions for the effective force acting on the monolayer as a function of the number particle number N .

As described in the supplement S1, the effective force acting on the monolayer,

$$F_{\text{eff}}(R) = -F_{\text{max}} \sin\left(\frac{2\pi R}{a}\right) \times \exp\left\{-\frac{2\pi^2}{a^2} \left[\sigma_x^2(R) + \frac{1}{3}\sigma_y^2(R)\right]\right\}, \quad (1)$$

is a function of the variances,

$$\sigma_\mu^2(R) = \delta_{y\mu} \frac{\bar{\mathbb{D}}_{yy}^{-1}(\mathbf{0}, R)}{N\beta} + \frac{1}{N\beta} \sum_{\mathbf{q} \neq \mathbf{0}} \bar{\mathbb{D}}_{\mu\mu}^{-1}(\mathbf{q}, R), \quad (2)$$

which are sums of the elements of the dynamical matrix

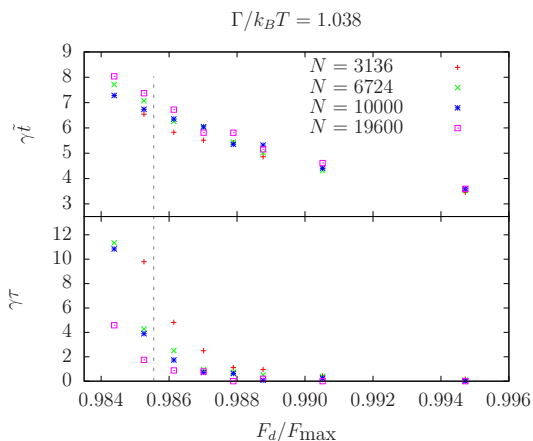


FIG. 8. Top: Average time the buildup phase plus the hopping wave takes to travel through the system as a function of the driving force F_d for different system sizes N . Bottom: Average time the system takes to nucleate a hopping wave also as a function of F_d and N . The dashed line is located at $F_{\text{max}}^{\text{eff}}$.

$\mathbb{D}(\mathbf{q})$ divided by the particle number. These variances can be interpreted as the mean value of the continuous

function $\bar{\mathbb{D}}(\mathbf{q}, R)$ discretized to N equally spaced points. The number of particles in the system determines how fine the “mesh” is. Naturally, the value of the variances converges as N becomes large and in the limit of infinitely large N , the sum over \mathbf{q} becomes an integral. According to our formula, the continuous function $\mathbb{D}_{\mu\mu}^{-1}(\mathbf{q}, R)$ has to be evaluated at the N \mathbf{q} -vectors compatible with a simulation of N particles. In order to trace the convergence of the solution to an infinitely large system, we have plotted, in Figure 7, our predictions for the effective force acting on the monolayer. Evidently, we considered a system size (indicated by a circle) which is quite close to the limit of an infinitely large system.

As was stated in the paper, the entire trajectory of the monolayer can be resolved into three times: the drifting time due to the effective substrate \tilde{t}_1 , the nucleation time τ , and the hopping wave time \tilde{t}_2 . The mean velocity of the monolayer is exactly equal to $\gamma v = a/(\tilde{t}_1 + \tilde{t}_2 + \tau) = a/(\tilde{t} + \tau)$. The time \tilde{t}_1 , which is the time that the monolayer needs to reach R_0 if $F_d < F_{\text{max}}^{\text{eff}}$ or $R = 0.25a$ if $F_d > F_{\text{max}}^{\text{eff}}$, can be calculated by evaluating the integral using the appropriate limits of integration,

$$\tilde{t}_1 = \int \frac{dR}{F_d + F_{\text{eff}}(R)} \quad (3)$$

and is independent of N in the manner discussed above. The hopping wave time is roughly $\tilde{t}_2 = a\sqrt{N}/v_{\text{wave}}(F_d)$, where $v_{\text{wave}}(F_d)$ is the velocity with which the radius of the hopping wave expands and is expected to monotonically increase with the driving force. The dependance on N stems from the fact that the hopping wave has to cover larger distances as the system size increases. Finally, the average nucleation time, τ is predicted to be proportional to the inverse system size $\tau \propto N^{-1}$ and scales exponentially in the free energy barrier associated with forming a critical cluster of hopping particles. This free energy barrier, in turn, depends on F_d and is expected to vanish if it exceeds $F_{\text{eff}}(R)$. Determining the exact functional form of these three times would require the determination of a series of proportionality terms, such as the kinetic prefactor, the surface tension due to a hopping wave, and the hopping wave velocity. Although this is feasible, such a detailed analysis is beyond the scope of this work and would be tantamount to solving the entire model in this parameter range. We are, nonetheless, able to make some predictions.

As a result of the aforementioned considerations, the mean velocity of the monolayer is predicted to scale very differently with the driving force and system size in the two dynamical regimes that were explored in this work. Since τ is minuscule or 0 in the thermal sliding regime, and most of the time is spent in the build up phase, \tilde{t}_1 determines the mean velocity. As a result, the expression $\gamma v = \sqrt{(F_d)^2 - (F_{\text{max}}^{\text{eff}})^2}$ is quite accurate in reproducing the velocity of the monolayer. In the nucleation regime,

the average nucleation time, τ , is the dominant time and therefore the velocity of the monolayer increases with system size and increases exponentially as F_d grows. In both regimes, the time the hopping wave takes to travel through the system scales with \sqrt{N} and F_d , but its contribution to the velocity is small since the other two times are much larger than \tilde{t}_2 . As a result we expect, that \tilde{t}

should *increase* slightly as the system size grows, whereas the nucleation time τ should *decrease* by a large amount for growing system sizes. Our expectations are confirmed in Figure 8. Finally, from the shape of the curves, the bottom panel also illustrates that the transition from nucleation dynamics to thermal sliding is continuous.